Numerical study of conductivity for the Anderson model in two and three dimensions

B. Kramer, A. MacKinnon, and D. Weaire*

Physikalisch-Technische Bundesanstalt, Bundesallee 100, 3300 Braunschweig, Federal Republic of Germany

(Received 25 June 1980; revised manuscript received 19 February 1981)

The equation-of-motion method is applied to the calculation of the conductivity for the Anderson model in two and three dimensions. The Kubo-Greenwood formula is evaluated by averaging suitable combinations of time-dependent states and extrapolating to the limit of infinite time. In agreement with earlier work we have found the critical value of the disorder parameter for a transition from localized to extended states to be $W/V = 6$ for the square lattice and $W/V = 15$ for the simple cubic lattice. No conclusion about the critical behavior of the conductivity near the Anderson transition was drawn because of rather large scatter in the data. The reasons for this scatter are discussed. It is concluded that statistically satisfactory information about the critical behavior of the conductivity can only be obtained from a numerical calculation for systems containing more than 10^5 sites in any dimension.

I. INTRODUCTION

The electronic properties of strongly disordered systems, such as amorphous solids, present a great challenge both to analytical theory and to numerical calculation. In particular, the problem of Anderson localization[1] has been attacked by a variety of analytical and numerical methods,[2] yet it remains controversial. Various criteria for localization have been used.[3] The one which is most closely related to experiment is the zero-temperature static electrical conductivity.[4] This is supposed to be *finite* if states at the Fermi level are *extended*, and *zero* if they are *localized*.

Unfortunately the conductivity is a comparatively complicated quantity to calculate and most early work concentrated on the localization length or the participation ratio, in attempting to discriminate between extended and localized states.[5] For simple tight-binding Hamiltonians some degree of consistency for the location of the Anderson transition was achieved in both two and three dimensions.[6] Increased interest in the calculation of the conductivity was generated by the continuing debate on its critical behavior. According to Mott,[7] there should be a discontinuous drop of the conductivity at the mobility edge (the energy which divides localized from extended states). Mott's picture, though not universally accepted,[8] has had much success in the interpretation of transport data from doped semiconductors,[9] amorphous solids,[4,10] and inversion layers.[11]

Licciardello and Thouless[12] were the first to claim to have accurately and rigorously calculated the conductivity in the vicinity of the Anderson transition. Their early results, together with some scaling arguments, led them to the conclusion that the value of the conductivity at the mobility edge (generally called the *minimum metal-*

lic conductivity, but this phrase has various shades of meaning) is a *universal* constant in two dimensions. Further calculations[13] yielded somewhat different results and caused these authors to largely withdraw from their former opinion, despite apparent experimental confirmation.[14,15]

The method of Licciardello and Thouless starts from the Kubo-Greenwood formula (see Sec. II). With certain assumptions, the conductivity is related to the change of individual eigenvalues when the boundary conditions are altered on a finite sample. Some of these assumptions have also been incorporated in a scaling argument by Abrahams et al.,[16] which leads to the startling conclusion that *all* states are localized in two dimensions for any disorder (but only weakly so for low disorder). This is consistent with arguments by Wegner,[17] starting from a disordered n-orbital model, and by Götze et al.,[18] using an approximate theory for the density response of particles moving in a random potential. Nevertheless, this conclusion is far from being universally accepted, and Lee,[19] in particular, has presented both analytical criticisms and numerical counter evidence.

In three dimensions, the above theories[16,17,18] do allow an Anderson transition but predict a zero minimum metallic conductivity. Meanwhile, further numerical methods for the calculation of conductivity have been developed. Prelovsek[20] has examined the diffusion of an electron released at $T = 0$ near the origin, with a wave packet made up of states close to a chosen energy. In this way he calculates the diffusivity which is simply related to the conductivity via the Einstein relation. His results seem to be consistent with an Anderson transition in both two and three dimensions, with a zero minimum metallic conductivity in both cases. Stein and Krey[21] have made a direct numerical evaluation of the Kubo-Greenwood formula

using a technique based on the recursion method. They conclude that their results are in favor of Mott's original suggestion. Lee's renormalization-group calculations,[19] already mentioned above, also indicate a finite minimum metallic conductivity in two dimensions.

In every case, the interpretation of the numerical results has proved difficult because it is necessary to make various extrapolations, of which the most obvious is that which takes the system size to infinity. Uncertainty arising from these extrapolations is difficult to quantify but seems enough in every case to obscure many of the delicate points at issue. Our own method, presented in this paper, is no exception. We shall try to be scrupulous in presenting enough results so that the difficulties regarding extrapolations can be appreciated.

We use the equation-of-motion method[22,23] to evaluate the Kubo-Greenwood formula for the conductivity.[24] The method can also be adapted to calculate other transport quantities. The content of the remaining sections is as follows.

In Sec. II the Hamiltonian is defined and the problem of the evaluation of the Kubo-Greenwood formula is stated. In Sec. III the equation-of-motion method is described and adapted to our present purpose. Section IV contains some remarks on the various extrapolations. Section V presents the results for the square and simple cubic lattices. Finally, Sec. VI contains a discussion of the results.

II. THE MODEL

In studies of this kind, it has become conventional to use the Anderson Hamiltonian with diagonal disorder. This is

$$H = \sum_{j=1}^{N} \epsilon_j \, |j\rangle\langle j| + V \sum_{j,j\Delta}^{N,Z} |j\rangle\langle j\Delta| \,, \qquad (1)$$

where the basis states $|j\rangle$ are located on the sites of a periodic structure. The elements ϵ_j are independent random variables, with a uniform distribution between $\pm\frac{1}{2}W$. The off-diagonal term couples each site j only to its Z nearest neighbors $j\Delta$ with constant matrix element V. The strength of disorder, represented by W, is usually scaled by the half-bandwidth of the system at zero disorder, being expressed as W/ZV.

It is generally felt that results on the Anderson transition for such a Hamiltonian should be qualitatively representative of a wide class of Hamiltonians. In the independent electron model, the conductivity at frequency ω is given by the Kubo-Greenwood formula

$$\sigma = \frac{2\pi e^2}{\hbar^2 m^2 \omega \Omega} \sum_{\alpha\beta} |\langle\alpha\,|\vec{\mathrm{e}}\cdot\vec{\mathrm{p}}\,|\beta\rangle|^2$$

$$\times \{f(E_\alpha)[1-f(E_\beta)]\delta(E_\alpha - E_\beta - \hbar\omega)$$

$$+ f(E_\beta)[1-f(E_\alpha)]\,\delta(E_\beta - E_\alpha - \hbar\omega)\}. \qquad (2)$$

Here Ω is the volume of the system, $\vec{\mathrm{e}}$ is the direction of the applied field, f is the Fermi-Dirac occupation function, α and β label energy eigenstates, and the other parameters have their conventional meanings.

This gives in the zero temperature, dc limit

$$\sigma_0 = \frac{2\pi e^2}{\hbar m^2 \Omega} \sum_{\alpha\beta} |\langle\alpha\,|\vec{\mathrm{e}}\cdot\vec{\mathrm{p}}\,|\beta\rangle|^2 \delta(E - E_\alpha)\delta(E - E_\beta). \qquad (3)$$

In our method, explained in the next section, σ_0 is calculated by a similar limiting process to that which leads from (2) to (3).

It remains to specify the matrix elements of the momentum operator $\vec{\mathrm{p}}$, which are essential to the evaluation of the Kubo-Greenwood formula. We shall use

$$\vec{\mathrm{p}} = -\frac{i}{\hbar}\, mV \sum_{j,j\Delta} \vec{\Delta}\, |j\rangle\langle j\Delta| \qquad (4)$$

as have others[12,21] before us. Here $\vec{\Delta}$ is the vector from site j to neighboring site $j\Delta$, that is

$$\vec{\Delta} = \vec{\mathrm{r}}_{j\Delta} - \vec{\mathrm{r}}_j \,. \qquad (5)$$

This is equivalent to the assumption that the position operator $\vec{\mathrm{x}}$ is diagonal in the site representation

$$\langle i\,|\vec{\mathrm{x}}\,|j\rangle = \delta_{ij}\vec{\mathrm{r}}_i \,, \qquad (6)$$

as may be shown using the commutation relation

$$\vec{\mathrm{p}} = \frac{im}{\hbar}\,[H,\vec{\mathrm{x}}]\,.$$

Substituting (4) into (3), we obtain for the Kubo-Greenwood formula the following expression, the evaluation of which is the object of our calculations

$$\sigma_0(E) = \frac{2\pi e^2}{\hbar\Omega}\, V^2 \sum_{jj'\Delta\Delta'} (\vec{\mathrm{e}}\cdot\vec{\Delta})(\vec{\mathrm{e}}\cdot\vec{\Delta}')$$

$$\times \sum_{\alpha\beta} \langle j\,|\,\alpha\rangle\langle\alpha\,|\,j'\rangle\langle j'\Delta'\,|\beta\rangle\langle\beta\,|\,j\Delta\rangle$$

$$\times \delta(E - E_\alpha)\delta(E - E_\beta). \qquad (8)$$

III. THE METHOD

Figure 1 summarizes the evolution of the equation-of-motion method to date. Originally developed by Alben et al. to calculate densities of states of disordered systems,[22] it was adapted by Weaire and Williams to calculate the average in-
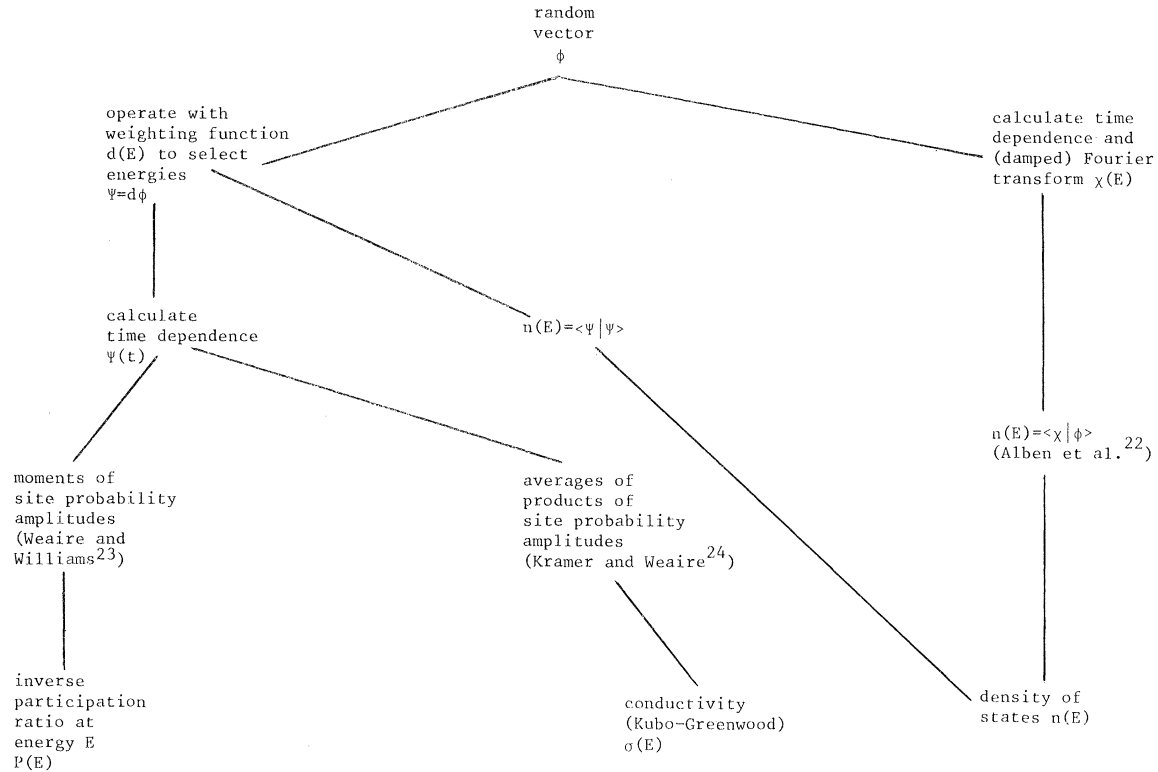
FIG. 1. Development of the equation-of-motion method for the calculation of properties of disordered systems.

verse participation ratio in order to study Anderson localization.[23] Kramer and Weaire showed how it could be further adapted to calculate the conductivity,[24] and it is with the details and results of this application that the present paper is concerned. We hope to clarify certain points in the other applications as well, particularly in the Appendix, which deals with statistical theorems which lie at the heart of this work.

In most applications of the method to date, we begin by defining *a random initial vector* on a finite sample of the lattice in question (usually with periodic boundary conditions). This may be written in terms of the basis functions of Sec. II as

$$|\phi\rangle = \sum_{j=1}^{N} a_j |j\rangle , \qquad (9)$$

where the site amplitudes a_j are independent random variables with a probability distribution independent of j.

We require that this distribution have the properties

$$\langle a_j \rangle_{\rm av} = 0 , \qquad (10)$$

$$\langle a_j a_j^* \rangle_{\rm av} = N^{-1} \delta_{jj'} , \qquad (11)$$

while the angle brackets here represents an en-

semble average for a single site. It is clear that it can equally well be taken to mean an average over sites in the limit of large N.

For the purposes of the calculation of the density of states (by either of the two methods indicated in Fig. 1) and the conductivity, the above properties are all that is required. However, it turns out that in the case of the calculation of the inverse participation ratio, further properties are needed (see the Appendix). These may be assured by choosing the real and imaginary parts of a_j to be normally distributed. In all of the work presented here we have made this choice.

The amplitudes of the vector (9) in the representation defined by the normalized energy eigenstates $|\alpha\rangle$,

$$a_\alpha = \langle \alpha | \phi \rangle , \qquad (12)$$

are also independent random variables with the same mean and mean square as the site amplitudes a_j. That is,

$$\langle a_\alpha \rangle_{\rm av} = 0 , \qquad (13)$$

$$\langle a_\alpha a_\beta^* \rangle_{\rm av} = N^{-1} \delta_{\alpha\beta} . \qquad (14)$$

For proof, see the Appendix.

We now operate upon the vector $|\phi\rangle$ with a function of the Hamiltonian designed to filter out its

energy components in a narrow range around some chosen energy E_0. In practice we use

$$d_m(H) = C_m[1 - E_{max}^{-2}(E_0 - H)^2]^m. \tag{15}$$

Here E_{max} is chosen so that the density of states lies entirely in the range $E \leq E_{max}$ and the normalization constant C_m is defined by

$$C_m^{-2} = \int_{-E_{max}}^{E_{max}} dx \left(1 - \frac{x^2}{E_{max}^2}\right)^{2m}. \tag{16}$$

This ensures that

$$\int_{-E_{max}}^{E_{max}} dx\, d_m^2(x) = 1. \tag{17}$$

Using such an operator we may define and calculate

$$|\Psi\rangle = d_m(H)|\phi\rangle. \tag{18}$$

In the energy representation this is

$$|\Psi\rangle = \sum_\alpha d_m(E_\alpha) a_\alpha |\alpha\rangle. \tag{19}$$

We will write it in the site representation as

$$|\Psi\rangle = \sum_{j=1}^N b_j(0)|i\rangle. \tag{20}$$

We proceed to calculate its time dependence and hence $b_j(t)$, using the time-dependent Schrödinger equation

$$i\hbar\frac{d|\Psi\rangle}{dt} = H|\Psi\rangle. \tag{21}$$

In doing so, we calculate the following combination of *time* averages (indicated by angle brackets):

$$\sigma_0^{m,N}(E) = \frac{2\pi e^2}{\hbar}\frac{N^2 V^2}{\Omega}$$

$$\times \sum_{jj'\Delta\Delta'} (\vec{e}\cdot\vec{\Delta})(\vec{e}\cdot\vec{\Delta}')[\langle b_j b_{j'\Delta}^* b_{j'\Delta} b_{j\Delta}^*\rangle_{av}$$
$$- \langle b_{j'} b_{j'\Delta'}\rangle_{av}\langle b_{j\Delta} b_j^*\rangle_{av}]. \tag{22}$$

We shall now show that the above is related to the Kubo-Greenwood formula (8) as follows. We first observe that, using (19) and (20), the time dependence of $b_j(t)$ may be written explicitly as

$$b_j(t) = \sum_\alpha d_m(E_\alpha) a_\alpha \langle j|\alpha\rangle e^{-(i/\hbar)E_\alpha t}. \tag{23}$$

This may then be substituted in (22). The only terms which survive are those in which the phase factors cancel inside the averages. It is clear that $E_\alpha = E_{\alpha'}$ only if $\alpha = \alpha'$, i.e., the eigenstates are nondegenerate for a disordered Hamiltonian. The expression in square brackets in (22) can thus be written

$$\sum_{\alpha\neq\beta} |a_\alpha|^2 |a_\beta|^2 \langle j|\alpha\rangle\langle\alpha|j'\rangle\langle j'\Delta'|\beta\rangle\langle\beta|j\Delta\rangle d_m^2(E_\alpha) d_m^2(E_\beta). \tag{24}$$

The two factors $|a_\alpha|^2$ and $|a_\beta|^2$ are independent random variables not correlated with any of the other factors in (24) and may hence be replaced by their mean values given by (14). We thus see that (22) is equivalent to

$$\sigma_0^{m,N}(E) = \frac{2\pi e^2 V^2}{\hbar\Omega} \sum_{jj'\Delta\Delta'} (\vec{e}\cdot\vec{\Delta})(\vec{e}\cdot\vec{\Delta}') \sum_{\alpha\neq\beta} \langle j|\alpha\rangle\langle\alpha|j'\rangle\langle j'\Delta'|\beta\rangle\langle\beta|j\Delta\rangle d_m^2(E_\alpha) d_m^2(E_\beta). \tag{25}$$

Finally, we see that

$$\lim_{m\to\infty} \lim_{N\to\infty} \sigma_0^{m,N}(E) = \sigma_0(E), \tag{26}$$

where σ_0 is defined by (8) since the d_m factors become delta functions at energy E in this limit. It is therefore necessary to perform calculations for large values of m and, preferably, to make a numerical extrapolation for $m\to\infty$. We are therefore confronted with three numerical extrapolations, in principle. For a given sample, time averages evaluated over a finite range of time must be extrapolated to infinity. Secondly, calculations must be performed for different sizes of the sample and extrapolated to infinite sample size. Thirdly (and only then), the above extrapolation $m\to\infty$ must also be made.

IV. EXTRAPOLATION OF THE DATA

To obtain meaningful results for the conductivity it is desirable to have some guidelines as to how

the quantity $\sigma_0^{m,N}(E)$ behaves when t, N, and m become very large. We shall discuss these in turn.

Substituting relation (23) into (22) we obtain for $\sigma_0^{m,N}(E)$ an expression of the form

$$\sigma_0^{m,N}(E) \sim \lim_{t\to\infty} \frac{1}{t}\sum_{\Delta E} A[\Delta E] \int_0^t dt' e^{-i\Delta E t'}$$
$$= \lim_{t\to\infty} f(t), \tag{27}$$

where ΔE are the differences between various eigenenergies and $A[\Delta E]$ is a product of amplitudes of the initial state and the eigenstates. In the limit $t\to\infty$ only the terms with $\Delta E = 0$ yield a nonzero contribution to the sum.

We investigate now how $f(t)$ behaves as a function of t. For very small $t(t^{-1} \gg W + ZV)$ almost all eigenstates contribute, and the two terms in Eq. (22) cancel. For large $t[t^{-1} \ll (W+ZV)/N]$ only the smallest ΔE contribute. This gives

$$f(t) = \sum_{\Delta E = 0} A[0] + \sum_{\Delta E \min} A[\Delta E_{\min}] \frac{1}{|\Delta E_{\min}|} \frac{1}{t}(1 - \sin|\Delta E_{\min}|t) + \cdots ,$$

(28)

where $\Delta E_{\min}$ denotes the smallest of the ΔE. Thus for large t we have

$$f(t) \approx \sigma_0^{m,N} + g \frac{1}{t} + c \frac{\sin|\Delta E|t}{|\Delta E|t} .$$

(29)

This suggests a plot of $f(t)$ as a function of t^{-1}. In practice, the oscillations give an idea about the error involved.

We were not able to derive any analytic relation for the behavior of the conductivity with the size of the system, N. Qualitatively, we expect in the localized regime a decrease in $\sigma_0^{m,N}$ for increasing N because more and more states, which seem extended for small systems, appear as confined to finite regions of space. In the extended regime $\sigma_0^{m,N}$ should stay roughly constant.

Finally we investigate the behavior with m. Taking the matrix elements in the conductivity as independent of α and β we have from Eq. (25)

$$\sigma_0^{m,N} \sim \left(\sum_\alpha d_m^2(E_\alpha)\right)^2 .$$

(30)

In the limit $N \to \infty$ we can replace the sum by an integral

$$\sigma_0^m \sim \left(\int dE\, n(E) d_m^2(E)\right)^2 .$$

(31)

Expanding the density of states in a Taylor series at the Fermi energy we obtain for large m [small width of $d_m(E)$]

$$\sigma_0^m \sim \sigma_0 + O\left(\frac{1}{m}\right).$$

(32)

This argument applies only to extended states. In the regime of localized states the momentum matrix elements are not independent of α and β. In analogy to the one-dimensional case[25] we would expect

$$\sigma_0^m \sim O\left(\frac{1}{\sqrt{m}}\right).$$

(33)

However, we found it difficult to derive this result along similar lines as for extended states.

V. NUMERICAL CALCULATIONS AND RESULTS

From the preceding discussion it appears necessary to use time cutoffs which are considerably larger than the inverse of the mean spacing between the energy levels of the system:

$$t \gtrsim N/(2ZV + W).$$

(34)

In our actual calculations we used up to $t \approx 1000$

V^{-1}. This should suffice for systems with up to 5000 sites.

The steplength in the numerical integration should be of the order of the inverse of the maximum energy difference occurring in Eq. (28), i.e.,

$$\Delta t_0 < (2ZV + W)^{-1} .$$

(35)

By virtue of the energy weighting function the effective bandwidth is decreased with increasing m. In order to save computer time we therefore take

$$\Delta t = \Delta t_0 (4m + 3)^{1/2}$$

(36)

as the steplength.

We have calculated $\sigma_0^{m,N}$ for the two-dimensional square lattice, and for the three-dimensional simple cubic lattice with periodic boundary conditions with finite m, N, and t. The Fermi energy was in the middle of the (symmetric) band, i.e., $E = 0$. The initial state was specified by using the probability distribution

$$p(a_j) = \frac{1}{2\pi} N |a_j| e^{-N|a_j|^2} .$$

(37)

For the integration of the time-dependent Schrödinger equation a standard Runge-Kutta subroutine was used.

An interesting test for our computer program is the case $m = 0$. From Eq. (25) we have

$$\sigma_0^{m=0} = \frac{e^2}{\hbar} \frac{4\pi}{a^{d-2}} \frac{1}{(2Z + W/V)^2}$$

(38)

because

$$d_0^2(E_\alpha) = \frac{1}{2ZV + W} \; ; \; -\left(ZV + \frac{W}{2}\right) < E_\alpha < \left(ZV + \frac{W}{2}\right).$$

(39)

Figures 2 and 3 show some results together with the values obtained from the relation (38). Data for $m \neq 0$ and various system sizes are shown in Fig. 4 for two dimensions, and in Fig. 5 for three dimensions.

For $t \to 0$, $\sigma_0^{m,N}$ tends to zero as expected from Eq. (22). With increasing t, $\sigma_0^{m,N}(t)$ becomes nonzero and fluctuates. For $W/V < 6$ in $2d$ (<15 in $3d$) the limiting values (for $t \to \infty$) are quite insensitive to m and N, whereas for $W/V > 6$ in $2d$ (>15 in $3d$) we have a decreasing trend when m and N are increased.

VI. DISCUSSION OF THE DATA

Trends in the time-extrapolated data can be followed more quantitatively if we try to trace the
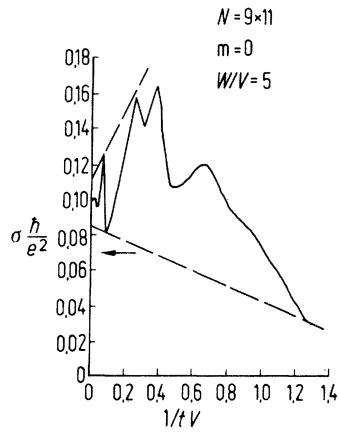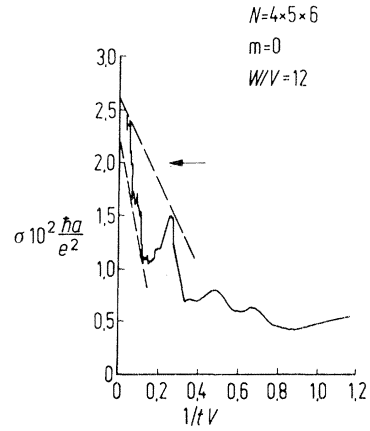
FIG. 2. Comparison of the result for the conductivity σ, in units of $e^2/\hbar$, obtained by extrapolating the time average of Eq. (22) with the analytical result for $m=0$ from Eq. (38) (position of arrow) for a square lattice with parameters $N = 9 \times 11$, and $W/V = 5$.

FIG. 3. Comparison of the result for the conductivity σ, in units of $e^2/\hbar a$, obtained by extrapolating the time average of Eq. (22) with the analytical result for $m=0$ from Eq. (38) (position of arrow) for a simple cubic lattice with $N = 4 \times 5 \times 6$ and $W/V = 12$.
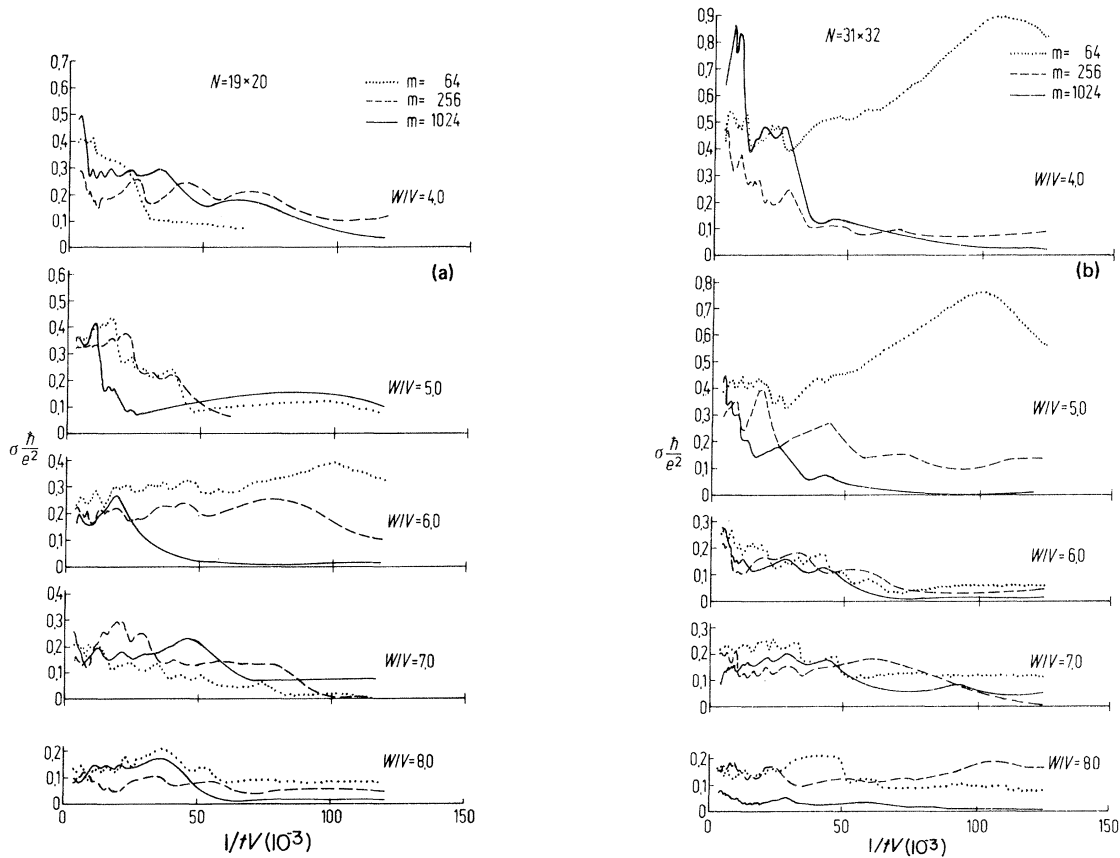
FIG. 4. Time averages of Eq. (22) for the square lattice denoted by σ, in units of $e^2/\hbar$ as a function of the reciprocal time cutoff $1/t$, in units of $V/10^3$ for $N = 19 \times 20$ (a), 31×32 (b), 47×41 (c), 70×71 (d), and disorder parameter W/V, and "width of delta function" m, as indicated in the figure. Fermi energy is in the center of the band.

results with increasing size of the systems, N, and the width of the weighting function, represented by m. Figures 6 and 7 show the dependence on the system size and on m.

Before attempting any interpretation a few general remarks are necessary. The energetic half-width of the weighting function is given by

$$\frac{\Delta E}{2E_{max}} = \frac{1}{2\sqrt{m}} \tag{40}$$

for large m. Therefore, the number of states contributing to the conductivity is approximately

$$n_{eff} \approx N \frac{1}{2\sqrt{m}}. \tag{41}$$

If we assume each state to contribute independently, the relative statistical accuracy of the conductivity is

$$\frac{\Delta \sigma}{\sigma} \approx \frac{1}{\sqrt{n_{eff}}} = \frac{2}{\sqrt{N}} (m)^{1/4}. \tag{42}$$

For $m = 256$, for instance, we obtain an energy resolution ΔE of roughly 3% of the total (Lifshitz)

bandwidth, which is in $2d$ about 0.5 V, and in $3d$ 0.9 V, approximately. On the other hand, the statistical accuracy for a system with 10^3 sites is roughly 18%.

It is clear that it would be of no use to increase the value of the time cutoff still more (and thus increasing the computer time) in order to reduce the uncertainty stemming from the time extrapolation, once a certain convergency stage has been reached. It is seen from Figs. 6 and 7 that in most cases the uncertainty from the time extrapolation is less or of the same order as the statistical uncertainty, which we expect from Eq. (42). Bearing all this in mind we observe a decreasing tendency of our results with N and m for $W/V \gtrsim 6$ and $W/V \gtrsim 15$ in $2d$ and $3d$, respectively. The behavior of the conductivity as a function of the disorder averaged over the largest system size used, and extrapolated with m (inserts), is shown in Figs. 8 and 9. The indicated error bars are estimated from the various extrapolations. Though we cannot conclude anything about the critical behavior of the conductivity from the results, we might conclude that an
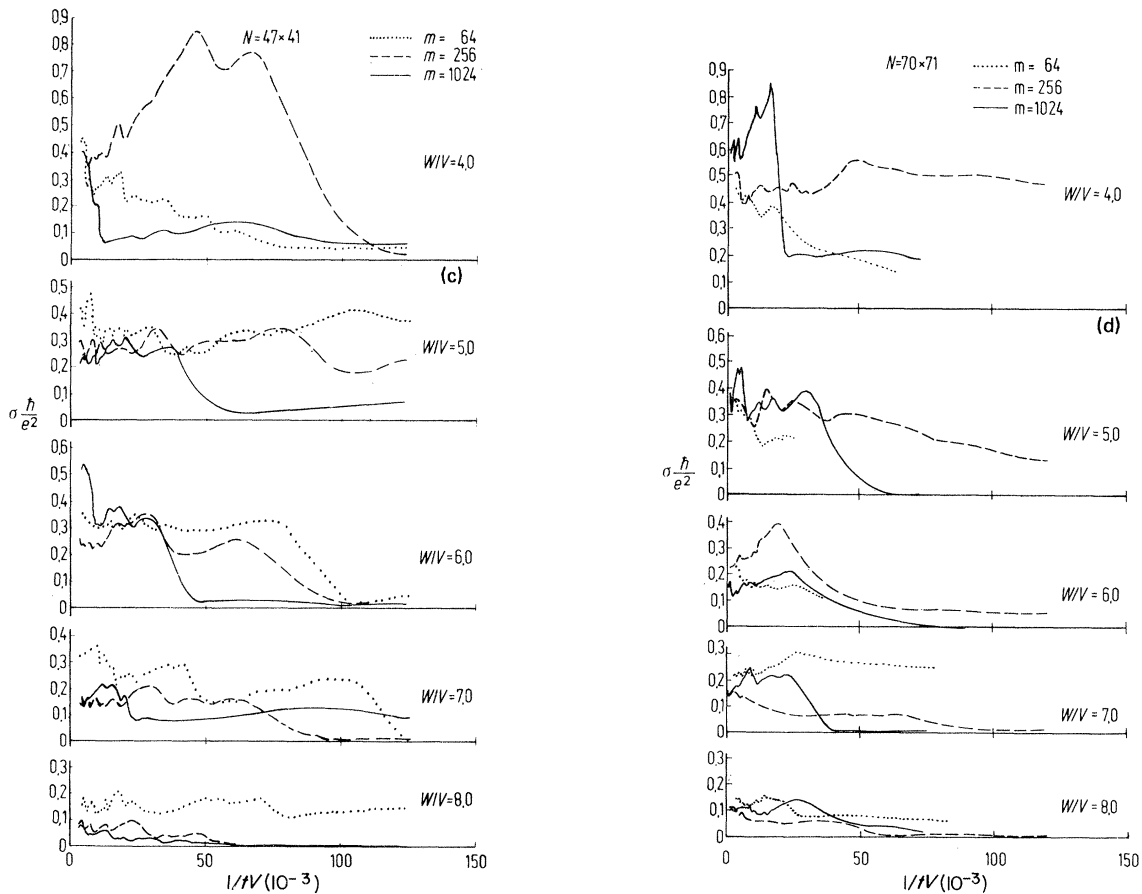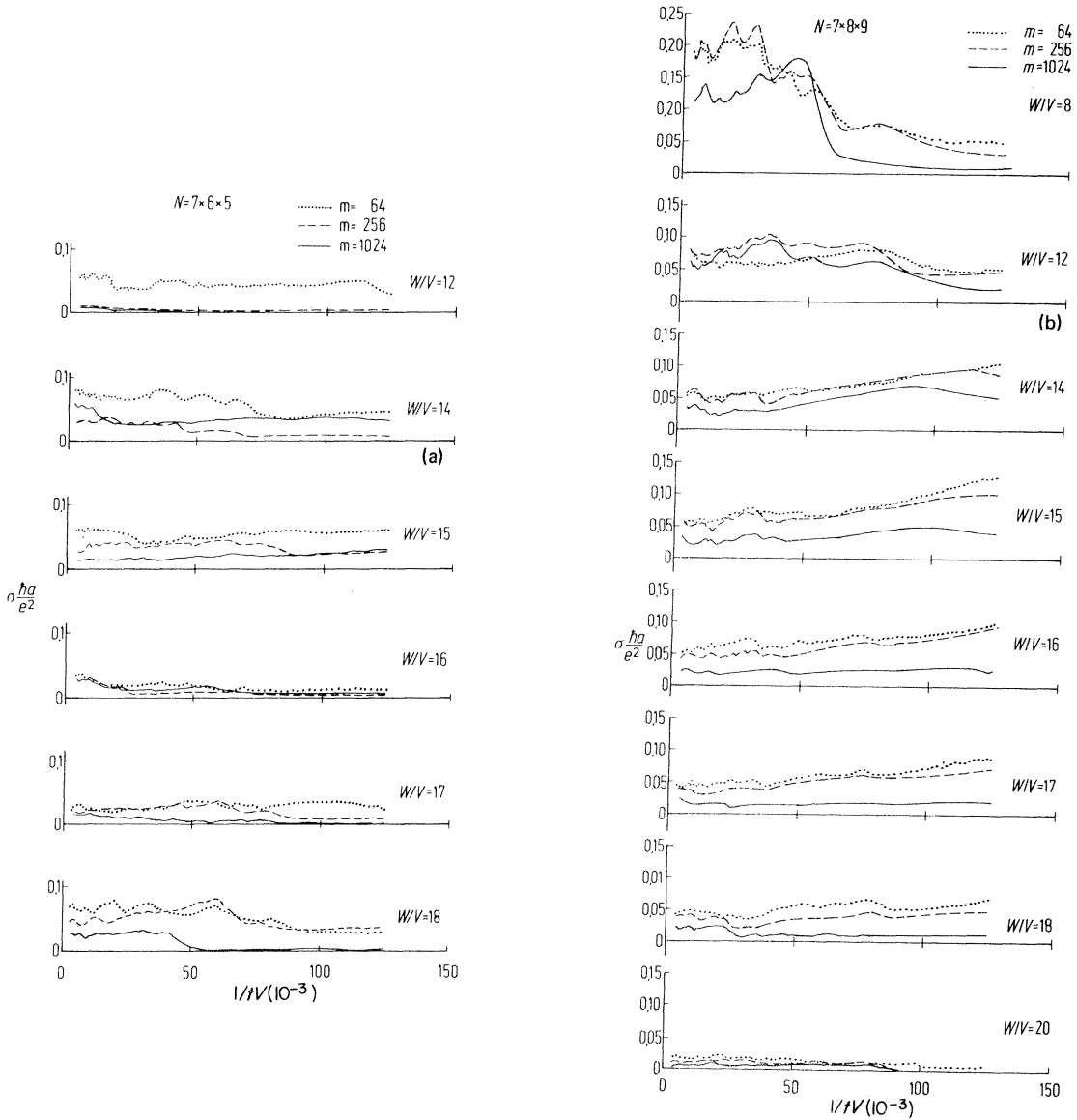

FIG. 4. *(Continued)*

FIG. 5. Time averages of Eq. (22) for the simple cubic lattice denoted by σ, in units of $e^2/\hbar a$ as a function of the reciprocal time cutoff $1/t$, in units of $V/10^3$, for $N = 7 \times 6 \times 5$ (a), $7 \times 8 \times 9$ (b), $11 \times 10 \times 9$ (c), $14 \times 12 \times 11$ (d), and disorder parameter W/V, and "width of delta function" m, as indicated in the figure. Fermi energy is in the center of the band.

Anderson transition takes place in both dimensions, the critical values of the disorder being $W_0/V = 6$ and $W_0/V = 15$ in $2d$ and $3d$, respectively, in agreement with earlier numerical work[19-21,26-28] (see also Table I).

However, this result may be questioned by a general argument. In order to draw any reliable conclusion regarding the Anderson transition it is necessary to make sure that the n_{eff} is such that the localized states no longer overlap. Thus

$$n_{eff}\lambda \ll N,\qquad(43)$$

where λ is the participation number of the states

at the Fermi level. Only under this condition is it possible to observe the trend towards zero conductivity in the localized regime. In particular, near the Anderson transition or in any other situation where the states are localized but very large, it is essential to consider very large systems in order to fulfill inequality (43) while maintaining an acceptable statistical accuracy. If we require an error of 10%, then from Eq. (42) we need $n_{eff} \approx 100$. For a system of 10^4 sites we can then observe a zero conductivity where λ is much less than 100. In two dimensions this implies a localization length of less than 10. Experience of one
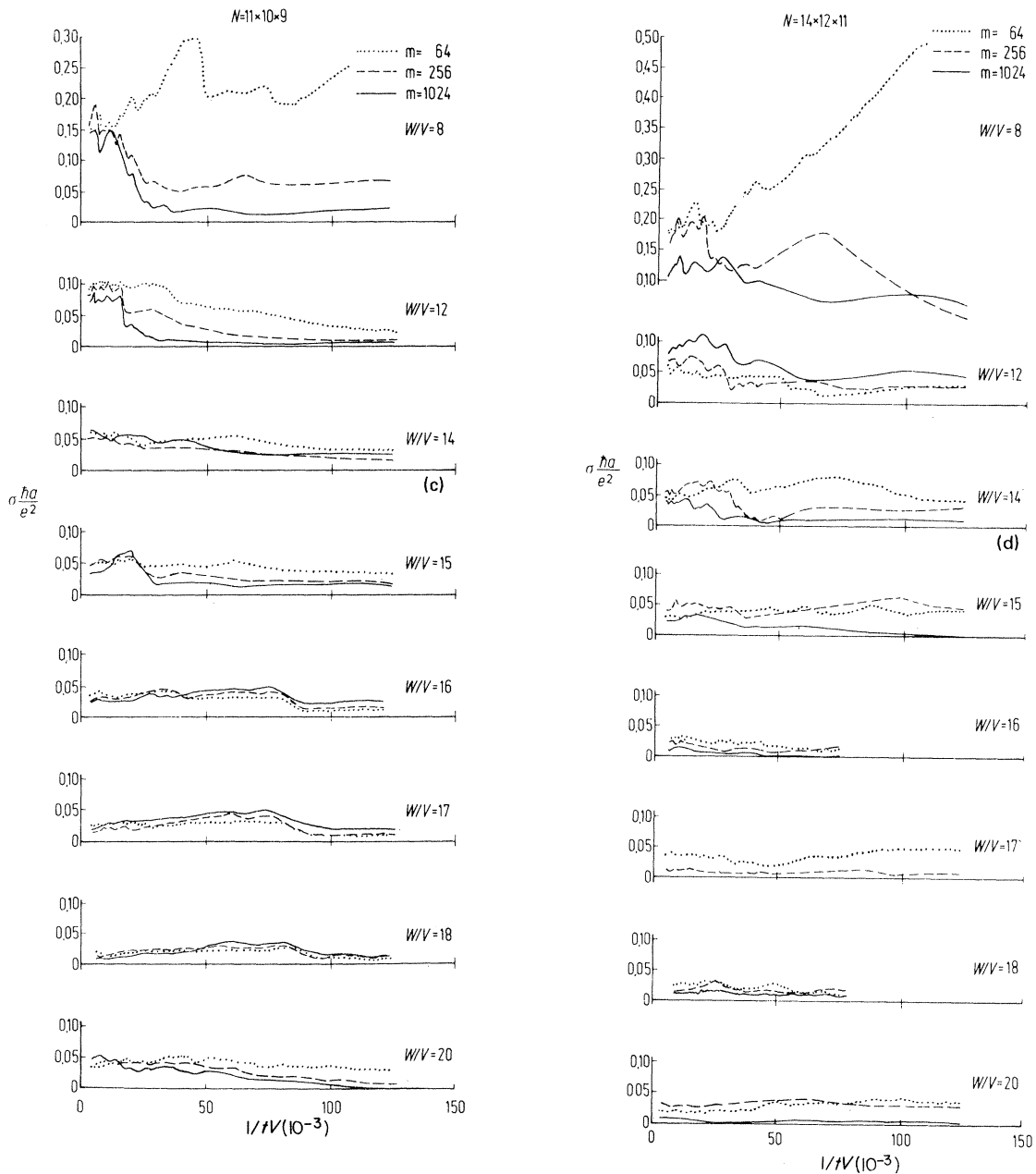
FIG. 5. (*Continued*)

dimension[25,29] shows that this might be far too small for any reliable conclusion about whether an Anderson transition takes place.

The above considerations apply not only to our method but to nearly all other current numerical methods[30] since none consider system sizes significantly greater than 10^4. Critical behavior will be observed in a plot of σ vs m near those values of disorder where inequality (43) is no longer fulfilled, i.e., as an effect of the maximum accessible system size.

VII. CONCLUSION

Though we are not in the situation of drawing any definite conclusion about the Anderson transition and the critical behavior of the conductivity from our data, we may deduce from Eqs. (40), (42), and (43) some condition for the values which the parameters m and N should take in order to make such a behavior detectable. First consider the question of the Anderson transition. If we want states with localization length 100 to be detected as localized, we need an energy resolution $\Delta E/$
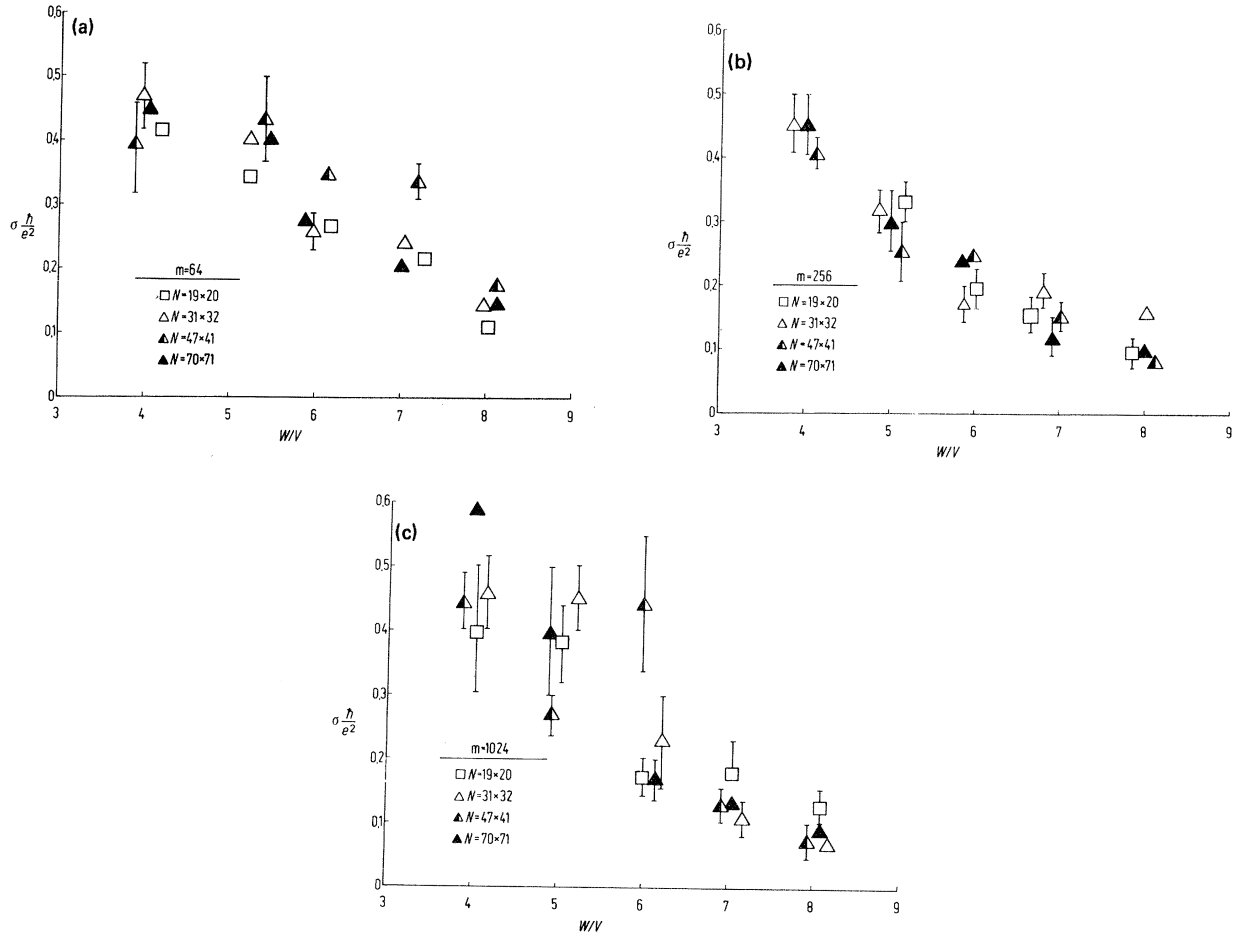
FIG. 6. Extrapolated time average of Eq. (22) for the square lattice denoted by σ in units of $e^2/\hbar$ as a function of the disorder W/V, for sizes of the system $N = 19 \times 20$ ($\square$), 31×32 ($\triangle$), 47×41 ($\blacktriangle$), 70×71 ($\blacktriangle$), and "width of delta function" $m = 64$ (a), 256 (b), 1024 (c). Fermi energy is in the center of the band. The error bars indicated are estimated from the oscillations with t in Fig. 4.

TABLE I. Comparison of the critical disorder for the Anderson transition obtained by various authors in two and three dimensions.

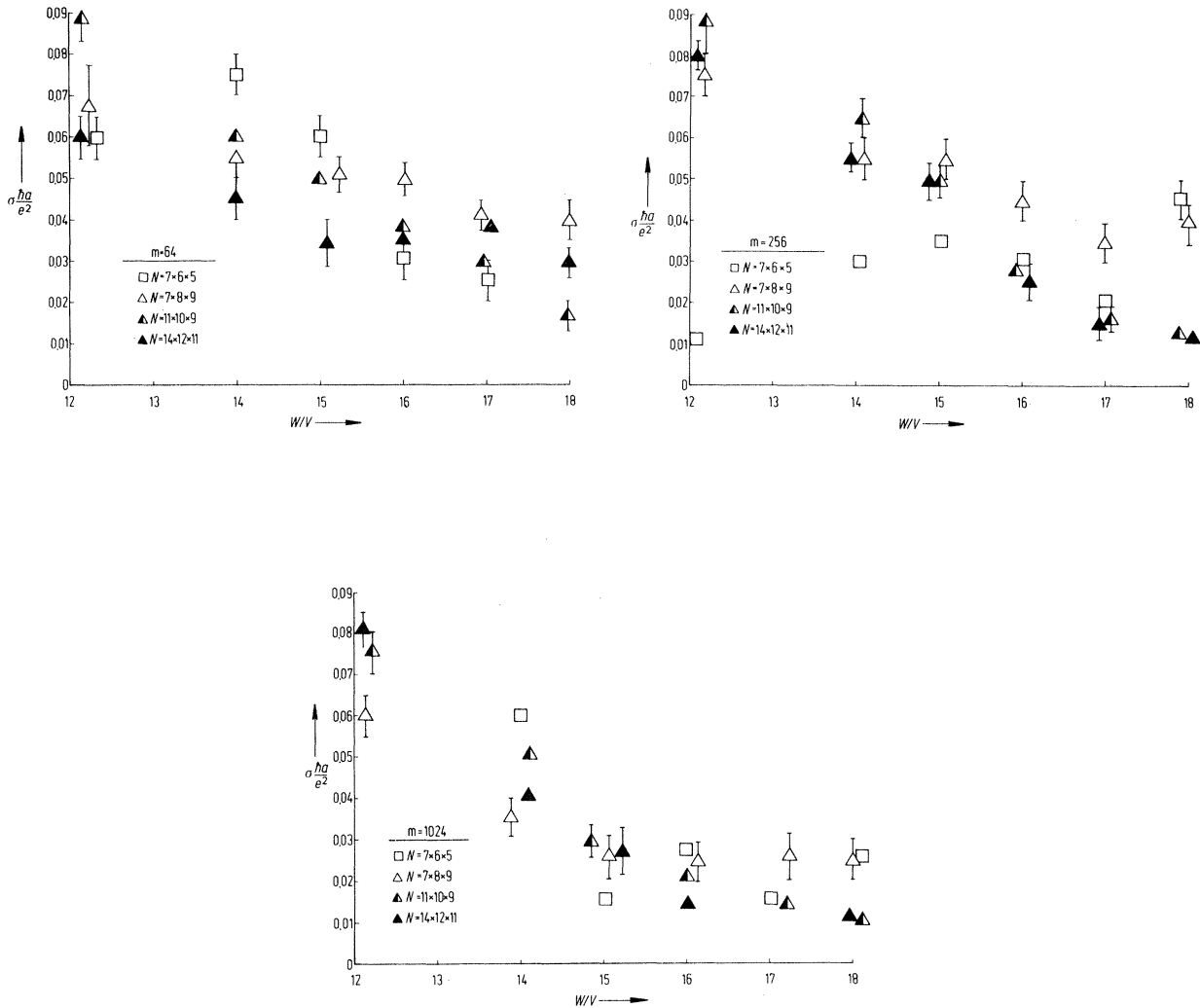| Dimension structure	This work	Lee (Ref. 19)	critical disorder W/ZV			
			Stein and Krey (Ref. 21)	Weaire and Srivastava (Ref. 27)	Prelovsek (Ref. 20)	Yoshino and Okazaki (Ref. 28)
$d = 2$ square lattice	1.5	1.45	1.6	1.5	1.6	1.6
$d = 3$ simple cubic lattice	2.5			2.5		
$d = 3$ diamond lattice			2.0	2.0	3.3	

FIG. 7. Extrapolated time averages of Eq. (22) for the simple cubic lattice denoted by σ in units of $e^2/\hbar a$ as a function of the disorder W/V, for sizes of the system $N = 7 \times 6 \times 5$ ($\square$), $7 \times 8 \times 9$ ($\triangle$), $11 \times 10 \times 9$ ($\blacktriangle$), $14 \times 12 \times 11$ ($\blacktriangle$), and "width of delta function" $m = 64$ (a), 256 (b), 1024 (c). Fermi energy is in the center of the band. The error bars indicated are estimated from the oscillations with t in Fig. 5.

$2E_{max} = n_{eff}/N = 10^{-2d}$, where d is the dimensionality. For a statistical accuracy of 10% we should have $n_{eff} = 100$ which would imply $N = 10^{2(d+1)}$. In order to obtain reliable information about the critical behavior of the conductivity we would need at least $N = 10^6$ sites in two dimensions and $N = 10^8$ in three dimensions. Even this may not be sufficient if the localization length is greater than 100 but less than infinity over a large range of disorder. The situation is more encouraging if we *know of the existence of an Anderson transition*, and want to detect the critical behavior of the conductivity:

If we require an energy resolution of 1% of the bandwidth we obtain $m = 2500$. Thus, concerning m our calculations are not far from being satisfactory. For a statistical accuracy of 1% we would need a system of $N = 10^6$ sites, keeping the energy resolution at 1%. In our opinion such accuracy requirements are presumably lower limits if we want to decide between a steplike and a square-root behavior of the conductivity, for instance. To our knowledge, none of the numerical methods used up to now for the conductivity meet even these latter (weaker) criteria, except in $1d$,
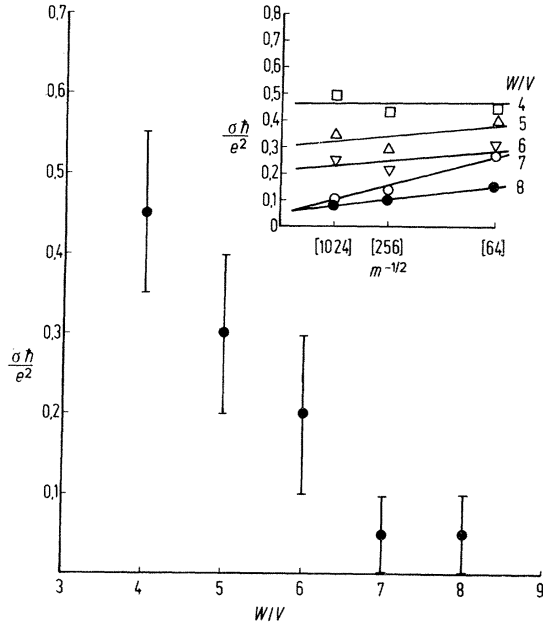
FIG. 8. dc conductivity σ as a function of the disorder W/V for the square lattice as obtained by averaging the values in Fig. 6 over the three largest systems for each value of m and extrapolating with $m \to \infty$ as shown in the insert, in which σ is plotted against $m^{-1/2}$. The corresponding values of m are shown in the brackets. The error bars are rough estimates from the various extrapolations.

where very recently a numerical procedure has been developed which allows for the treatment of systems up to 10^9 sites.[25]

APPENDIX

The statistical theorems which we require are quite elementary, but it seems desirable to explain them fully to avoid misunderstanding. The first is related to the familiar rule of the addition of variances in statistics.

Theorem 1

If $\vec{X}$ is a vector whose elements are independent random complex variables, each of which is of mean zero and variance σ^2 (the mean of its squared modulus), and U is a unitary matrix, the vector $\vec{y} = U\vec{X}$ is also composed of independent random variables with mean zero and variance σ^2. This may be simply proved as follows:
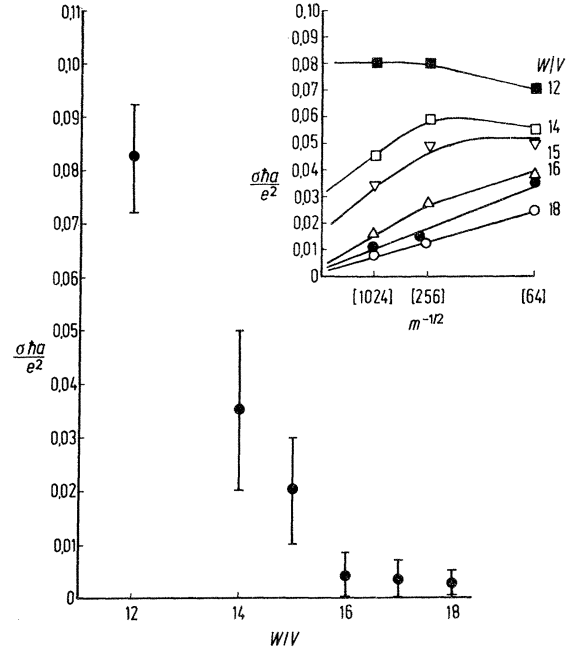

FIG. 9. dc conductivity σ as a function of the disorder for W/V for the simple cubic lattice as obtained from the values shown in Fig. 7 by the same procedure as for the square lattice. The inset shows σ as a function of $m^{-1/2}$. The values of m are shown in the brackets. The error bars are rough estimates from the various extrapolations.

The jth element of $\vec{y}$ is

$$y_j = \sum_i U_{ji} X_i . \tag{A1}$$

Taking the mean of both sides we have

$$\langle y_j \rangle_{av} = \sum_i U_{ji} \langle X_i \rangle_{av} = 0 . \tag{A2}$$

The mean of a product of the new variables is

$$\langle y_j^+ y_{j'} \rangle_{av} = \sum_{ii'} U_{ji}^+ U_{j'i'} \langle X_i^+ X_{i'} \rangle_{av}$$

$$= \sum_{ii'} U_{ji}^+ U_{j'i'} \langle |X_i|^2 \rangle_{av} \delta_{ii'}$$

$$= \sigma^2 \sum_i U_{ji}^+ U_{j'i}$$

$$= \sigma^2 \delta_{jj'} . \tag{A3}$$

The new variables are therefore independent, with variance σ^2.

These results are used in Sec. III to relate the statistical properties of amplitudes of a random vector in the site and energy representations. The unitary matrix in question is that which is made up of eigenvectors of the Hamiltonian and hence transforms any given vector from the site

representation to the energy representation. The properties of normal distributions include a much stronger theorem related to the central limit theorem.

Theorem 2

If $\vec{X}$ is a vector whose elements are independent complex variables, each of which has independent normally distributed real and imaginary parts with mean zero and variance $\frac{1}{2}\sigma^2$, and U is a unitary matrix, the elements of $\vec{y} = U\vec{X}$ are similarly distributed independent random variables. (The factor of $\frac{1}{2}$ in the variance is included for consistency with the notation in theorem 1.)

The proof of this theorem is as elementary as for the above. The probability distribution for one element of $\vec{X}$ is

$$\frac{1}{2\pi\sigma^2} \, e^{-|X_i|^2/\sigma^2} , \tag{A4}$$

multiplying probabilities for its real and imaginary parts. The probability distribution for the entire vector is

$$p_1(\vec{X}) = \left(\frac{1}{2\pi\sigma^2}\right)^N e^{-|\vec{X}|^2/\sigma^2} , \tag{A5}$$

where N is the number of components in the vector.

Since the Jacobian of a unitary transformation is everywhere unity, the probability distribution of the vector $\vec{y}$ is

$$p_2(\vec{y}) = p_1(\vec{X}) = \left(\frac{1}{2\pi\sigma^2}\right)^N e^{-|\vec{y}|^2/\sigma^2} \tag{A6}$$

since $|\vec{X}|^2 = |\vec{y}|^2$, the transformation being unitary.
This may be written as

$$p_2(\vec{y}) = \prod_{i=1}^{N} \left(\frac{1}{2\pi\sigma^2}\right) e^{-|y_i|^2/\sigma^2} . \tag{A7}$$

Since the probability factorizes in this way, the individual components y_i are seen to be independent and to have the same distribution as each of the original X_i variables.

In the derivation of formulas for the inverse participation ratios (of which the lowest is the mean fourth power of the site amplitudes of eigenfunctions) this theorem was invoked, since the means of higher powers of the amplitudes in the energy representation are required in that case. If we begin with general site-amplitude distribution these are not known, but for the special case of a normal distribution, Theorem 2 can be used. For example,

$$\langle |\vec{y}|^4\rangle_{\rm av} = \langle |\vec{X}|^4\rangle_{\rm av} = 2\sigma^4 , \tag{A8}$$

which was used in the evaluation of the inverse participation ratio.[23] To avoid confusion in comparison with previous work it should be pointed out that a complex variable with this distribution may also be defined to have random phase and an *exponential* distribution of squared modulus.

---

*Present address: Dept. of Physics, University College, Belfield, Dublin, Ireland.

[1]P. W. Anderson, Phys. Rev. **109**, 1492 (1958).

[2]B. Kramer and D. Weaire, in *Amorphous Semiconductors*, edited by M. H. Brodsky (Springer, Berlin, 1979), p. 9.

[3]K. Ishii, Prog. Theor. Phys. Suppl. **53**, 77 (1973).

[4]N. F. Mott and E. A. Davis, *Electronic Processes in Noncrystalline Solids* (Oxford University Press, London, 1971).

[5]D. J. Thouless, Phys. Rep. **13**, 93 (1974).

[6]D. Weaire and B. Kramer, J. Non-Cryst. Solids **35 & 36**, 9 (1980).

[7]N. F. Mott, Philos. Mag. **26**, 1015 (1972).

[8]M. H. Cohen and J. Jortner, Phys. Rev. Lett. **30**, 699 (1973); Phys. Rev. A **10**, 978 (1974).

[9]A recent collection of results is published in the Proceedings of the International Conference on Impurity Bands in Semiconductors, Wurzburg, 1979, special issue of [Philos. Mag. B **42**, 725 (1980)].

[10]N. F. Mott, in *The Metal Non-Metal Transition in Disordered Systems*, edited by L. R. Friedman and D. P. Tunstall (SUSSP, Edinburgh, 1978), p. 149.

[11]M. Pepper, Contemp. Phys. **18**, 423 (1977).

[12]D. C. Licciardello and D. J. Thouless, J. Phys. C **8**, 4157 (1975).

[13]D. C. Licciardello and D. J. Thouless, J. Phys. C **11**, 925 (1978).

[14]R. C. Dynes, J. P. Garno, and J. M. Rowell, Phys. Rev. Lett. **40**, 479 (1978).

[15]M. Pepper, in *The Metal Non-Metal Transition in Disordered Systems*, edited by L. R. Friedman and D. P. Tunstall, (SUSSP, Edinburgh, 1978), p. 285.

[16]E. Abrahams, P. W. Anderson, D. C. Licciardello, and T. V. Ramakrishnan, Phys. Rev. Lett. **42**, 673 (1979).

[17]R. Oppermann and F. Wegner, Z. Phys. B **34**, 327 (1979); F. Wegner, *ibid*. **35**, 207 (1979).

[18]W. Götze, J. Phys. C **12**, 1279 (1979). W. Götze, P. Prelovsek, and P. Wölfle, Solid State Commun. **30**, 369 (1979).

[19]P. A. Lee, Phys. Rev. Lett. **42**, 1492 (1979).

[20]P. Prelovsek, Solid State Commun. **31**, 179 (1979); Phys. Rev. B **18**, 3657 (1978).

[21]J. Stein and U. Krey, Z. Phys. B **37**, 13 (1980).

[22]R. Alben, M. Blume, H. Krakauer, and L. Schwarz,

Phys. Rev. B 12, 4090 (1975).

[23]D. Weaire and A. R. Williams, J. Phys. C 10, 1239 (1977).

[24]B. Kramer and D. Weaire, J. Phys. C 11, L5 (1978).

[25]A. MacKinnon, J. Phys. C 13, L1031 (1980).

[26]D. Weaire and B. Kramer, J. Non-Cryst. Solids 32, 131 (1979).

[27]D. Weaire and V. Srivastava, in *Amorphous and Liquid Semiconductors*, edited by W. Spear (CICL,

University of Edinburgh, 1977), p. 286.

[28]S. Yoshino and M. Okazaki, J. Phys. Soc. Jpn. 43, 415 (1977).

[29]G. Czycholl and B. Kramer, Z. Phys. B 39, 193 (1980).

[30]Exceptions are the real-space renormalization procedures and decimation methods are used by P. A. Lee [Phys. Rev. Lett. 42, 1492 (1979)] and Hideo Aoki [J. Phys. C 13, 3369 (1980)]. It seems, however, difficult to calculate the conductivity with these methods.